

Article

Environmental Fate of Trace Elements in Depositional Sediments after Flashflood Events: The Case of Mandra Town in Greece

Paraskevi Maria Kourgia^{1,2}, Ariadne Argyraki^{1,*} , Vasiliki Paraskevopoulou² , Fotini Botsou² , Efstratios Kelepertzis¹ and Manos Dassenakis²

¹ Department of Geology and Geoenvironment, National and Kapodistrian University of Athens, Panepistimiopolis, Zographou, 15784 Athens, Greece; bkourgia@geol.uoa.gr (P.M.K.); kelepert@geol.uoa.gr (E.K.)

² Laboratory of Environmental Chemistry, Department of Chemistry, National and Kapodistrian University of Athens, 15784 Athens, Greece; vparask@chem.uoa.gr (V.P.); fbotsou@chem.uoa.gr (F.B.); edasena@chem.uoa.gr (M.D.)

* Correspondence: argyraki@geol.uoa.gr

Abstract: Flash floods are one of the harshest natural hazards, having a wide range of substantial impacts for human and environmental health in the short-term and long-term. On 5 November 2017, a high-intensity storm caused a catastrophic flash flood event in the town of Mandra, a western, outer suburb of the Athens Metropolitan Area in Greece. In this study, we determine the aqua regia extractable concentrations of trace elements in residual sediments and associated soils after the flash flood and evaluate the fractionation of contaminants in geochemical compartments. Geochemical data are coupled with physicochemical parameter measurements and mineralogy to identify possible factors explaining the variability of trace element concentrations, while a dilute acid extraction is used to monitor changes of the reactive fraction of the trace elements over the term of 1 year following the flood event. Aqua regia concentrations in flood-deposited sediments reached values of 1 mg/kg (Cd), 24 mg/kg (Co), 183 mg/kg (Cr), 599mg/kg (Cu), 1080 mg/kg (Mn), 195 mg/kg (Ni), 122 mg/kg (Pb) and 945 mg/kg (Zn). Multivariate statistical techniques classified the elements according to their natural or anthropogenic origin. Trace elements of geogenic origin (As, Co, Cr, Mn, Ni) dominate in flood deposited material. The cluster of anthropogenic elements (Cd, Cu, Pb, Zn) shows significant correlation with total organic carbon and magnetic susceptibility, while a significant seasonal variation has been observed for total organic carbon, Cd and Mn contents in the deposited sediments. Results allow a better understanding of the distribution of elements in the surface cover during and after catastrophic events in urban areas and provide useful information on the long-term exposure of the residents.

Keywords: environmental geochemistry; natural disasters; flooding; surface runoff



Citation: Kourgia, P.M.; Argyraki, A.; Paraskevopoulou, V.; Botsou, F.; Kelepertzis, E.; Dassenakis, M. Environmental Fate of Trace Elements in Depositional Sediments after Flashflood Events: The Case of Mandra Town in Greece. *Sustainability* **2022**, *14*, 2448. <https://doi.org/10.3390/su14042448>

Academic Editor: Guido Paliaga

Received: 30 December 2021

Accepted: 18 February 2022

Published: 21 February 2022

Publisher's Note: MDPI stays neutral with regard to jurisdictional claims in published maps and institutional affiliations.



Copyright: © 2022 by the authors. Licensee MDPI, Basel, Switzerland. This article is an open access article distributed under the terms and conditions of the Creative Commons Attribution (CC BY) license (<https://creativecommons.org/licenses/by/4.0/>).

1. Introduction

Flash floods are one of the harshest natural hazards with a wide range of tangible and intangible impacts that can be both short-term and long-term [1–5]. In the Mediterranean region, flooding becomes an increasingly significant issue [6] as population expands to river deltas and coastal areas that are subjected to inundation mostly from small rivers [7] and ephemeral mountain torrents [8–12]. Furthermore, due to climate change, it is expected that extreme precipitation events and flooding will be increasing in the future [13–15]. In addition to acute catastrophic consequences such as loss of human lives and property damage, floods play a significant role in the transport of trace elements associated with particulate matter, especially in severely polluted catchments. In such watercourse systems, both concentrations of suspended particulate matter and pollutant contents increase with

the growing discharge, particularly in the early stage of flooding [9,11], [13,16–20]. Their values can remain high in the surface environment even during the flood attenuation causing long term health effects that are not well documented [21].

Trace elements can follow different pathways leading from their source to their receptors, with potential impacts on human health. Specifically, floods play a central role in modifying the dispersal pollutant patterns in a catchment. During a flood event, the pollutants formerly temporarily stored in natural or artificial drainage channels are quickly transferred to floodplains [20,22]. Recently deposited sediments may easily release trace elements during resuspension with increasing flow velocity, while flooding events may also cause primary pollution with extreme precipitation causing failures of settling ponds or washes from stockpiles [19]. In the long term, extensive mud deposits left in some areas have the potential to act as sources of airborne contaminants and be a potential hazard for the health of local communities [23]. Inhabitants of flood-impacted areas may be exposed to Potentially Toxic Elements (PTEs) through the oral, respiratory or dermal pathways. Risks are maximized in communities living near flood-impacted industrial or agricultural areas [21,23]. Flooded agricultural areas have also been demonstrated to be affected by heavy metal pollution [24], after flooding. Furthermore, studies simulating flooding conditions *ex situ* have demonstrated that the inundation of floodplain soils remobilizes trace elements [22,25]. The ultimate receptor of flood run-off and suspended particulates is the marine environment where shallow estuarine and coastal areas can be impacted by metal pollution causing potentially harmful effects on the marine ecosystem [8,26,27].

Greece has been affected by flooding since ancient times [9], as evidenced by anti-flooding works of the Minoan and Mycenaean eras (c. 2000–1050 BC). On 15 November 2017, a high intensity convective storm, leading to precipitation of 300 mm in 13 hours in the center zone of the incident, hit the western, outer suburbs of the Athens Metropolitan Area in Greece, causing a disastrous flash flood in the town of Mandra (population 12,888). The event caused 24 fatalities, and was the deadliest flood in the country since the 1970s. The catastrophic phase of flooding and its immediate consequences have been systematically studied by Diakakis et al. [1,10] in terms of flood characteristics including flood extent, maximum water levels and peak discharge estimations as well as flood impacts in different aspects of the human and natural environment. However, what remained within deposited sediment in the aftermath of this event remains unknown. Therefore, there is a need to assess the long-standing exposure of the returning residents to flood-related contaminants such as PTEs, potentially posing a substantial health hazard through accidental contact of Mandra residents with the deposited sediment. During the catastrophic phase of the flash flood event, vehicles, electrical transformers and various chemicals originating from households and local industries were dispersed throughout the streets of Mandra and were accumulated throughout the affected neighborhoods (Figure S1). Areas that were unaffected by the debris flows and rapidly moving water were covered by depositional sediments after the flood.

Considering the significance of depositional sediments as pollutant accumulators and their potentially toxic impact on aquatic and atmospheric environments and human health [28,29], the present study was conducted to assess the content of PTEs in the surface soil and flood-deposited sediment in Mandra town. The specific research objectives were to: (i) determine the contribution of natural versus anthropogenic elemental sources in the flood deposited sediment and associated soil; (ii) study the fractionation of PTEs in different compartments of the flood sediments; and (iii) identify seasonal changes in the reactive elemental fraction of the trace elements by comparing post-storm results over the term of one year following the flood event.

2. Materials and Methods

2.1. Study Area and Sample Collection

The town of Mandra is situated between the west end of the Athens Metropolitan Area and the southeast foothills of Mt Pateras (1132 m) (Figure 1). The study area has

generally flat topography. During the last 5 decades, following industrialization, Mandra changed from a residential–agricultural area to a mixed-land-uses area (i.e., residential, agricultural, and industrial). Different types of industries, including oil refineries, steel facilities, cement factories, petroleum recycling units, an industry of munitions, large warehouses, oil distribution facilities, and many chemical industry facilities, are located in the wider area between the two major towns of the plain, Elefsina and Aspropyrgos [30].

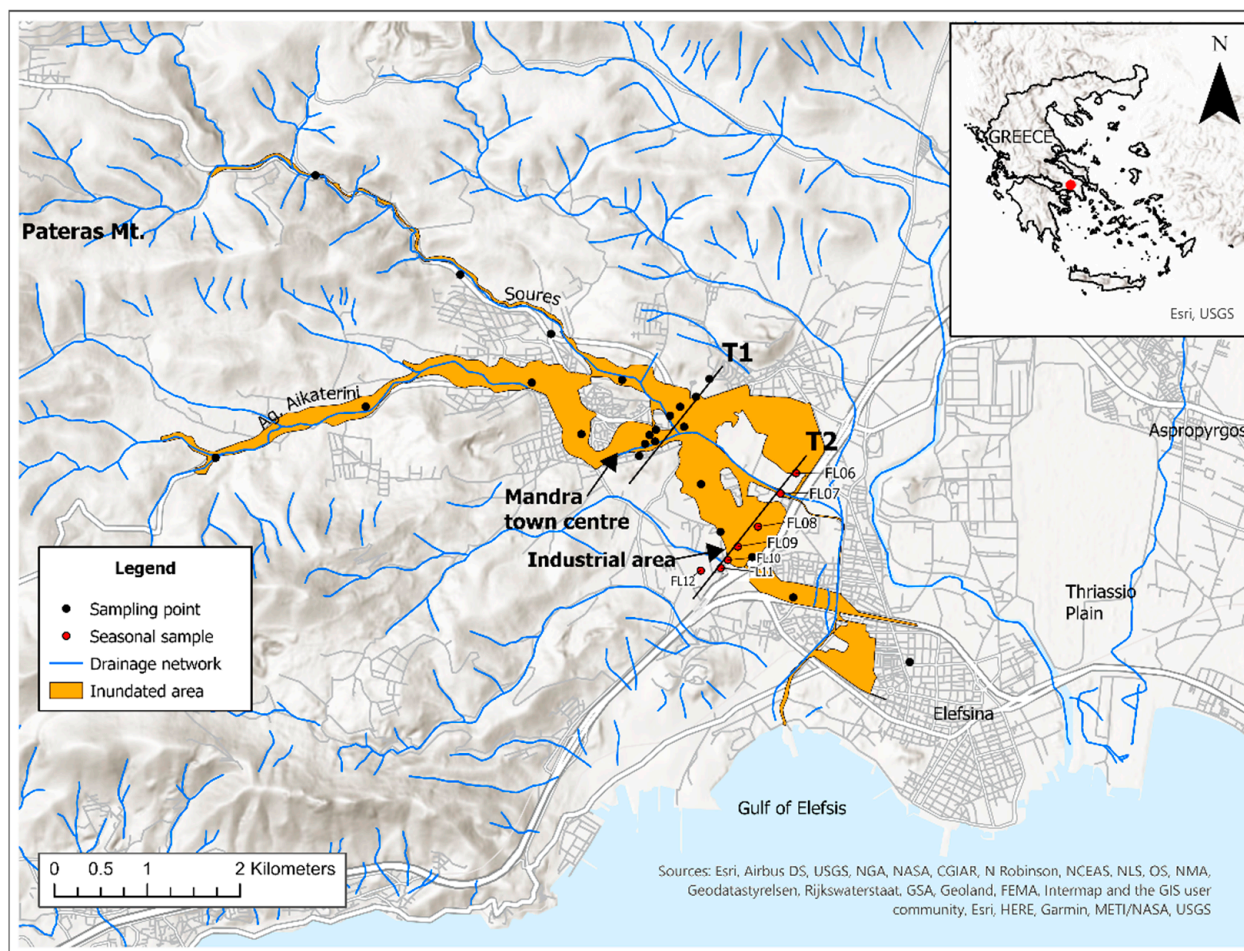


Figure 1. Map of the study area showing sampling locations, sampling traverses (T1, T2) and extent of inundated area after Diakakis et al. [1]. The study area is indicated by the red dot on the insert map of Greece.

Geologically, the study area is characterized by an east–west trending ridge mainly consisting of Middle to Upper Triassic limestone, dolomitic limestone and dolomite rock (Figure S2). These formations are strongly karstified and at locations they form an irregular basement for brown-red bauxites [31,32]. Bauxite ore is described as brown-red, mostly of boehmitic soluble type with pisolitic texture. Red clays (terra rossa) are sometimes intercalated between bauxite and the overlying limestones, while small lenticular bauxitic layers appear within the limestone cover [31]. The broader area is characterized by the presence of active fault zones [33]. Geomorphologically, the area is characterized by the sharp relief of Mt. Pateras, drained by ephemeral torrents. This results in steep topography and increased vulnerability to landslide erosion on hillslopes [1].

A total of 30 samples of unconsolidated material, either flood-deposited sediment (20 samples) or soil from non-flooded locations (10 samples), were collected three weeks after the flash flood event, 6 December 2017, along the drainage path of the two tributaries (Sours and Agia Aikaterini) (Figure 1). A total of 15 of the samples were collected upstream and downstream from the junction of the tributaries to reveal the distribution of the trace

elements. Another 15 samples were collected along two traverses cutting through the flood flow: Traverse 1 (T1) crossing at the town center of Mandra; and Traverse 2 (T2) crossing at the industrial area. This sampling strategy was selected in order to present a cross section of residential–commercial (T1) and industrial (T2) areas and be able to compare elemental contents in the flood sediments in the respective areas of Mandra. For a better understanding of the controlling factors of PTEs in the industrial area, additional samples were collected seasonally, 4 times per year in the year following flooding along T2. All samples of 1–1.5 kg each were collected with a PVC spatula at a depth of approximately 0–5 cm. The presence of PTEs and resulting health issues by accidental exposure through oral, respiratory, or dermal pathways have mostly been studied in the surface soil cover (0–5 cm) [29,34]. It is noted that no soil-core samples were collected, because the assessment of downwards migration of PTEs was not included in the objectives of the present study. Examples of sample collection sites are shown in Figure S1 of the Supplementary Material.

2.2. Preparation for Analysis and Laboratory Methods

2.2.1. Determination of Physicochemical Parameters

All samples were transported to the laboratory in plastic zip-lock bags and were dried at a constant temperature of 50 °C for 3 days in an air-dry oven. Subsequently, they were gently disaggregated and sieved to <2 mm to remove coarse material. Representative portions of each depositional sediment sample were further sieved through a nylon 70- μ m sieve and kept at an ambient temperature (15–20 °C). Major physicochemical properties including pH, total organic carbon (TOC), magnetic susceptibility and grain size distribution (sand, silt, clay) were determined. Soil pH was measured after mixing the <2 mm sample fraction with deionized water (1:2.5 (w/v)) [35]. Total organic carbon (TOC%) was determined on the <70 μ m fraction by loss on ignition (LOI) in a muffle furnace at 500 °C for 24 h [36]. Magnetic susceptibility (χ) was measured on 10 mL, <70 μ m fraction samples using a Bartington Magnetic Susceptibility Meter (model: MS2B) with a dual-frequency sensor according to a procedure described elsewhere [37]. Further information on magnetic measurements is provided in the Supplementary Material. Grain size distribution (vol.%) in the sand, silt and clay fractions was determined using the hydrometer sedimentation method applied on the coarse fraction (<2 mm) of the samples [38].

2.2.2. Mineralogical Analysis and Scanning Electron Microscopy Study

Qualitative mineralogical analysis was performed by X-ray diffraction (XRD) using a Siemens D5005 X-ray diffractometer, applying Cu K α radiation at 40 kV and 40 nA, in 0.020° steps at 1.0 step intervals. Scanning Electron Microscopy–Energy Dispersive Spectrometry (SEM-EDS) was carried out on carbon-coated soil/ sediment grains, by a Jeol JSM 5600 SEM instrument, equipped with an Oxford ISIS 300 microanalytical device. The high-density (specific gravity >2.96) fraction of selected samples was subjected to SEM-EDS study in the backscatter electron (BSE) mode in order to identify trace element hosting phases.

2.2.3. Chemical Analysis Methods

Chemical analysis was performed on the <70 μ m fraction, previously demonstrated to be a relevant grain size for assessing environmental risk in urban areas [39]. The near-total content of PTEs was determined in hot (95 °C) aqua regia (HNO $_3$ -HCl) digested samples by ICP-MS. The results were used to calculate the reactivity ratio or percent reactivity. Solutions were made to final volume of 10 ml with deionized water, and were analyzed for 33 chemical elements. This study focused on the analytical results of PTEs, i.e., As, Cd, Cu, Co, Cr, Ni, Mn, Pb, Zn for environmental purposes and some major elements (Al, Ca, Fe, Mg) to aid the interpretation of mineralogy. Analytical duplicates, in-house reference materials and reagent blanks were included for the quality control program. The modified Community Bureau of Reference (BCR) protocol was applied to evaluate the trace element fractionation in the 7 samples collected along T2 in the industrial area

with successive extractions by 0.11 M acetic acid, 0.5 M hydroxylammonium chloride in 0.05 M nitric acid (reducing agent) and 1 M ammonium acetate at pH 2 after digestion with 8.8 M hydrogen peroxide (oxidizing agent) [40]. The specific samples were selected because they yielded the highest concentrations of Pb and Zn according to the aqua regia dissolution. A final step using a HNO₃-HCl mixture was included to dissolve the residue after the three extraction steps. All elemental concentrations were measured by Flame Atomic Absorption Spectroscopy (FAAS), except Cd which was measured by Graphite Furnace Atomic Absorption Spectroscopy (GFAAS). The recovery rates for each chemical element were estimated by comparing the sum of the four fractions with the aqua regia digestion results (see quality control section in Supplementary Material).

The reactive forms of trace elements in the same 7 samples from T2 were extracted by a dilute acid (0.43 M HNO₃) leaching at ambient [41]. The same procedure was applied to the seasonal samples collected from the same sites. Concentrations of Pb, Zn, Cu, Ni, Cr, Co and Mn were measured by FAAS and concentrations of Cd by GFAAS.

2.3. Statistical Analysis and GIS

The MINITAB 17 software was used for statistical analysis. Data and geochemical maps with spatial distributions of PTEs concentrations, in the depositional sediments and soils of the studied area were compiled in a geographical information system (GIS) (ArcGIS Pro). The GIS included geospatial information (georeferenced sampling points, simplified lithological map, topography, extent of inundated area [1]) and land use data from the Corine land cover database [42]. Graduated size symbols were used for data posting maps of aqua regia extractable concentrations of the studied trace metals and other parameters (pH, % TOC and χ). The natural breaks method, based on the histogram of each variable, was adopted to define the concentration classes.

3. Results

3.1. Physical Characteristics and Magnetic Susceptibility of Soils and Sediments

The key physicochemical properties of the samples are presented in Table 1. The samples are weakly alkaline, with medium to high equivalent calcium carbonate content. The TOC content varies widely in the samples (1.5–4.9%), while in terms of grain size distribution the fine fraction dominates with percentages of clay, silt and sand of 5.9–24%, 65–84% and 0.6–22%, respectively. The measured magnetic susceptibility values (χ), indicate that the samples are dominated by a ferrimagnetic component. The χ values of less than $0.1 \times 10^{-6} \text{ m}^3 \text{ kg}^{-1}$ are indicative of dominating antiferromagnetic or paramagnetic components [43]. The samples yielded an average χ value of $1.99 \times 10^{-6} \text{ m}^3 \text{ kg}^{-1}$, which is 20 times over $0.1 \times 10^{-6} \text{ m}^3 \text{ kg}^{-1}$ indicating the predominance of secondary ferrimagnetic minerals. A significant statistical relationship was identified between the geochemical and mineral magnetic data (see below), suggesting that there is a link between magnetite-like phases and trace metals (Cu, Cd, Pb and Zn) in the Mandra environment.

Table 1. Statistical summary of physicochemical properties, magnetic susceptibility (χ) and aqua regia extractable concentrations of major and trace elements for the collected samples (n = 30). Median total concentrations of some studied elements in the soils of the neighboring Thriassio plain as determined in previous study of Massas et al. [30], are provided for comparison.

Parameter	Mean	Median	Minimum	Maximum	Standard Deviation	Median of Thriassio soil [30]
pH	8.00	8.03	7.27	8.36	0.24	8.0
TOC (%)	2.80	2.74	1.45	4.93	0.95	2.86
Sand (%)	6.29	4.29	0.57	21.7	5.8	50.9
Silt (%)	78.9	79.5	64.6	84	4.27	27.6
Clay (%)	14.9	13.9	5.93	23.5	4.82	21.5
χ ($10^{-6} \text{ m}^3/\text{kg}$)	1.99	1.97	1.09	3.03	0.39	
Al (%)	2.04	2	0.86	3.19	0.63	
As (mg/kg)	10.9	11	6	15	2.21	

Table 1. Cont.

Parameter	Mean	Median	Minimum	Maximum	Standard Deviation	Median of Thriassio soil [30]
Ca (%)	12.3	12.1	2.49	24.6	4.73	
Cd (mg/kg)	0.70	0.70	0.25	1.1	0.16	
Co (mg/kg)	18.2	18	8	24	4.17	24
Cr (mg/kg)	93.6	89.5	58	183	24	
Cu (mg/kg)	53.6	31.5	19	599	104	37.8
Fe (%)	2.75	2.72	1.53	3.86	0.61	1.6
Mg (%)	1.31	1.23	0.7	2.53	0.43	
Mn (mg/kg)	739	742	350	1080	171	320.8
Ni (mg/kg)	133	134	64	195	32.4	81.1
Pb (mg/kg)	49.9	40	24	122	25.8	111.8
Zn (mg/kg)	170	106	52	945	186	154.6

3.2. Mineralogical Composition of the Samples

Mineral phases commonly found in the samples include calcite, dolomite, quartz, illite, albite, clinochlore and other subordinate clay minerals (Figure 2). Calcite is one of the most abundant minerals in most of the examined samples, reflecting the effect of the limestone bedrock. Quartz, the most resistant mineral to physical and chemical weathering, is also abundant in the samples. Trace amounts of illite and clinochlore were also identified by XRD. No significant differences were observed in the XRD patterns of the seasonal samples. It is noted, however, that the performed mineralogical analysis is only qualitative and although the relative abundance of mineral phases in the samples may vary seasonally, this could not be verified in this study, given the limitations of our interpretation and the variation between the collected samples.

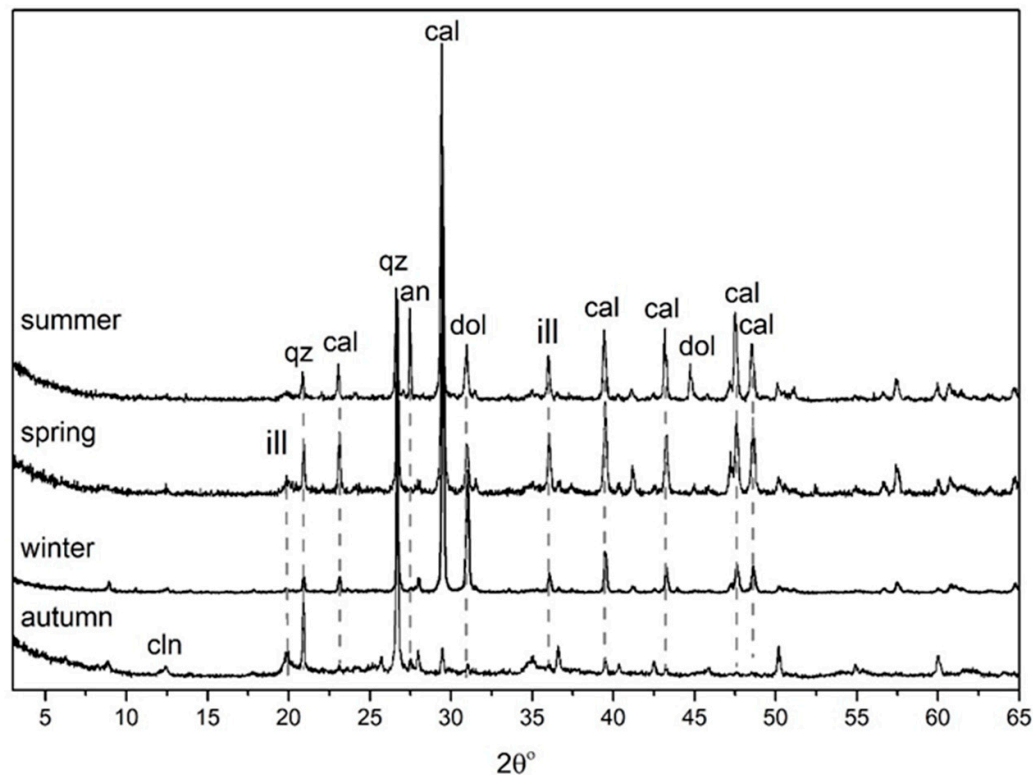


Figure 2. Typical example of XRD patterns of seasonal samples collected from the same location on T2 (industrial area). No significant change in mineralogy has been observed over the course of 1 year after the flash flood. (cln = clinochlore, ill= illite, qz= quartz, cal = calcite, an = anorthite, dol = dolomite).

The SEM-EDS study of selected samples revealed the presence of grains rich in PTEs such as (Cu, Zn)-oxide phases, as well as magnetite spherules which are typically formed by combustion processes in urban environments [28] (Figure 3 and Table S1).

3.3. Geochemical Characterization of Soil and Depositional Sediment Samples

3.3.1. Aqua Regia Extractable Trace Elements

The elemental concentrations after aqua regia digestion of the total samples are summarized in Table 1. Of the PTEs, Zn, Mn and Cu are the elements that display the greatest variation, with concentration ranges of 52–945 mg/kg, 350–1080 mg/kg and 19–599 mg/kg, respectively. All elements show a wide range in their concentration values reflecting the contribution of the flood in the investigated area. In terms of median values, Mn, Ni and Zn display the highest concentrations in aqua regia analysis. Median values of the studied elements follow the decreasing order of Ca > Fe > Al > Mg > Mn > Ni > Zn > Cr > Pb > Cu > Co > As > Cd. Compared to a previous study by Massas et al. [30], considered to be a good representation of the local soil geochemical baseline as it was performed in the adjacent area of Thriassio Plain, levels of Pb, Cu and Zn in the present dataset are considerably lower. Contrarily, the Mn median concentration displays an over two-fold increase in the present study. A further striking difference compared to the Thriassio soil study is the significantly higher silt content of samples of the present study, reflecting the effect of the flash-flood event on the related depositional sediment.

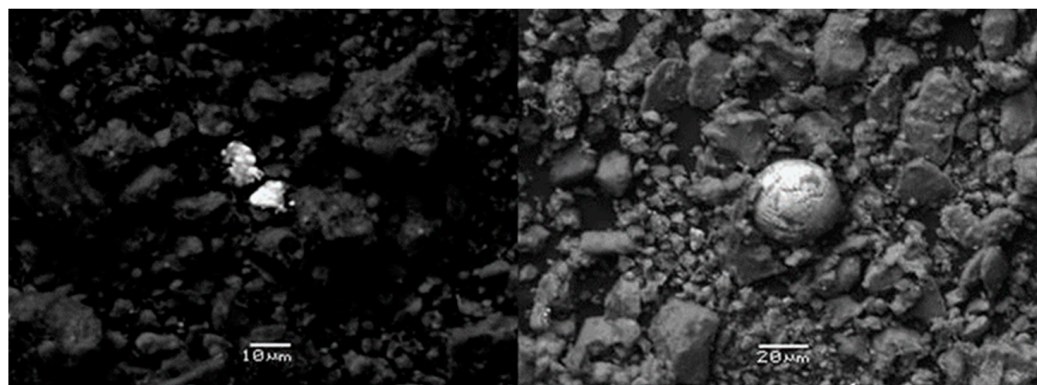


Figure 3. SEM photomicrographs of samples FL06 and FL08 from T2 crossing the industrial area of the town of Mandra. **Left:** bright grains enriched in Cu (45.20%) and Zn (33.48%). **Right:** magnetite spherule. Darker grains are mainly carbonate and aluminosilicate minerals.

A comparison of PTE contents in samples collected within and outside the flooded area revealed that maximum values correspond to sampling points within the flooded area for all elements (Figure 4); however, differences were found to be statistically significant only for Co and Ni (ANOVA, $p < 0.05$).

In order to group the studied trace elements and to identify possible common sources, a hierarchical cluster analysis was performed on elemental concentrations and other parameters measured in the samples, using the weighted pair-group average based on Pearson correlation coefficients [43]. The results are presented graphically in the dendrogram of Figure 5. Two distinct clusters are identified based on a criterion of similarity of over 50%, whereas pH forms a separate cluster. The first cluster is divided into multiple subclusters and contains % clay, Ni, Fe, Mn, Co, As and Cr. The second cluster includes %TOC, χ , Cu, Pb, Zn and Cd, and is subdivided into two subgroups; χ , Cd and Pb are clustered in one subgroup and Cu, Zn and %TOC in a second subgroup. The magnetic susceptibility (χ) presents similarity of over 75% with Cd and Pb. A correlation between %TOC and Cu-Zn is observed, indicating an apparent relationship of these parameters.

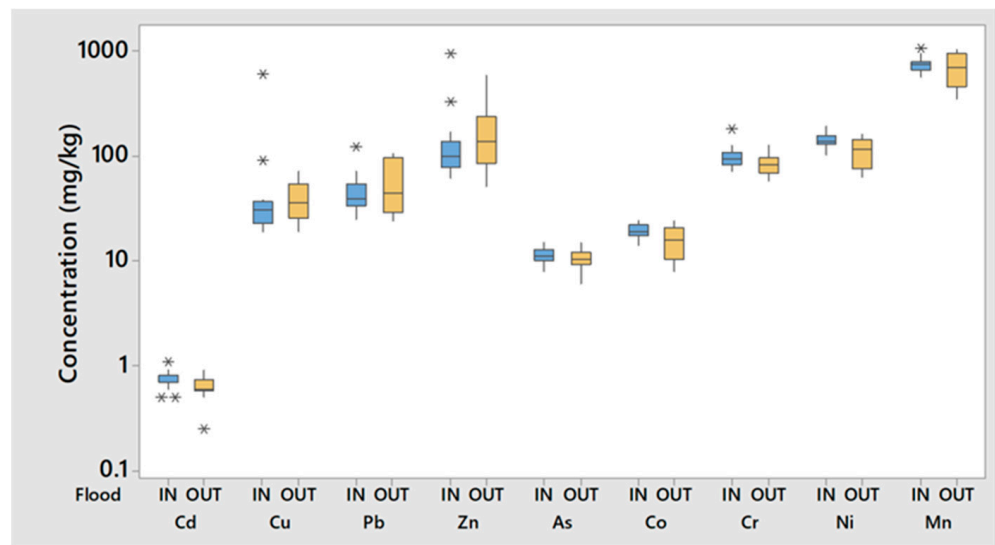


Figure 4. Boxplot comparison of aqua regia extracted trace element concentrations from within (n = 20) and outside (n = 10) the flooded area.

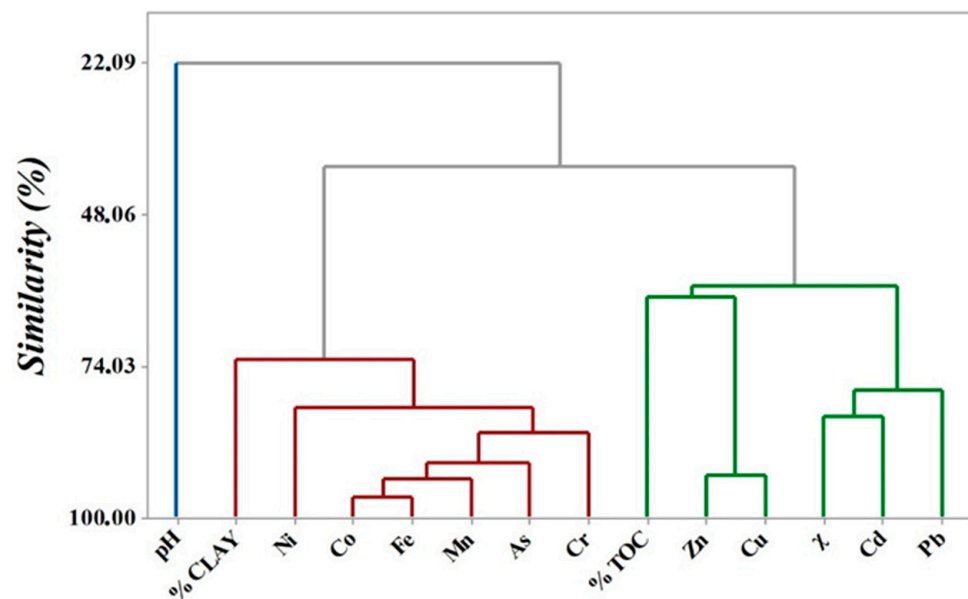


Figure 5. Hierarchical clustering results (dendrogram) of the measured parameters after aqua regia extraction (n = 30).

In order to further explore the controlling factors of elemental associations, factor analysis was performed on aqua regia extracted elemental concentrations, pH, %TOC, %clay content and magnetic susceptibility (χ). The factor analysis results are presented in Table 2.

Three factors are identified, accounting for 78% of the total variance. The first factor accounts for 43.1% of the total variance, and includes %clay, Ni, Co, Fe, Mn, As and Cr with positive loadings. The second factor controls 19.9% of the total variance and includes %TOC, χ , Pb and Cd with negative loadings. In the present study, magnetite spherules, which are typical products of combustion processes [28,44] have been identified in the urban samples during the SEM-EDS analysis (Figure 3). The third factor, accounting for 14.8% of the total variance contains Cu and Zn with high positive loadings. This is further supported by the SEM-EDS results (Figure 3, Table S1), where some of the grains appear to be rich in these two trace elements.

Table 2. Total variance explained and matrix of Varimax rotated factor loadings and communalities for elemental concentrations extracted by aqua regia and physicochemical soil parameters.

Variable	Factor 1	Factor 2	Factor 3	Communality
pH	−0.406	0.219	−0.474	0.437
TOC	−0.072	−0.716	0.169	0.546
Clay	0.771	0.201	0.113	0.647
χ	0.444	−0.793	0.039	0.828
Cu	0.132	−0.112	0.941	0.916
Pb	−0.190	−0.825	0.288	0.799
Zn	−0.144	−0.427	0.871	0.961
Ni	0.863	0.023	0.112	0.758
Co	0.976	−0.012	0.012	0.954
Mn	0.926	0.002	−0.035	0.859
Fe	0.950	−0.223	0.035	0.953
As	0.892	−0.252	0.151	0.882
Cd	0.361	−0.658	0.197	0.602
Cr	0.785	−0.362	−0.004	0.747
Variance	6.035	2.783	2.072	10.8893
% Cumulative variance	0.431	0.199	0.148	0.778

3.3.2. Sequential Extraction Results and Reactive Trace Element Concentrations

The chemical partitioning patterns of the investigated elements according to the modified BCR sequential extraction procedure in the 7 depositional sediments of T2, collected 1 month after the flash flood, are shown in Figure 6. The results are expressed as percentage distributions of the elements within each fraction. The elemental fractions were evaluated to provide a first approximation of the potential metal mobility and bioaccessibility of PTEs in the collected samples. The first fraction corresponding to water-soluble, easily exchangeable and carbonate-related forms is interpreted as the most mobile and bioaccessible in the environment [45]. Fraction 2 corresponds to elements bound to Fe and Mn oxides and fraction 3 corresponds to elements complexed with sulfides and organic matter. Fraction 2 can be mobilized with increasing reducing conditions and fraction 3 with increasing oxidizing conditions. As a result, the sum of the first three steps of the sequential extraction (F1 + F2 + F3) is considered as the potentially labile fraction, whereas the residual forms of metals are unavailable for transport, plant uptake or be bioaccessible to humans [46].

Copper in the depositional sediments was mainly concentrated in the residual (62%) and oxidizable phases (24%) and showed a weaker association with the reducible (10%) and exchangeable phases (5%), except for one sample which reached percentages of 44% in the reducible and 8% in the exchangeable phase, respectively. Lead was strongly associated with the oxidizable and residual phases in most samples with smaller amounts in the reducible and exchangeable fractions (24% and 10%, respectively). The percentage of exchangeable Pb fraction was found to be significantly high for sample FL09 (16%). The chemical association of Zn was dominated by reducible/specifically adsorbed (32%) and residual (41%) phases, with the oxidizable (19%) and exchangeable (9%) fractions being of secondary importance. The exchangeable Zn phase was notably high (18%) in sample FL10. Cadmium in the depositional sediments was the most vulnerable PTE to mobilization with a high percentage (41%) extracted in the initial steps of exchangeable/specifically adsorbed fraction. High percentages of Co (6–44%) and Mn (35–66%) were also related to the labile fraction with concentrations ranging from 8 to 24 mg/kg for Co and 750 to 1080 mg/kg for Mn. The chemical partitioning of Mn was dominated by the reducible phase. A significant contribution of the residual fraction was found for Co, probably indicating that some Co may be held in acid soluble, phyllosilicate minerals. The operational speciation of both Ni and Cr was governed by the residual species in the sediments with extraction percentages reaching 80–90% during the strong acid dissolution stage.

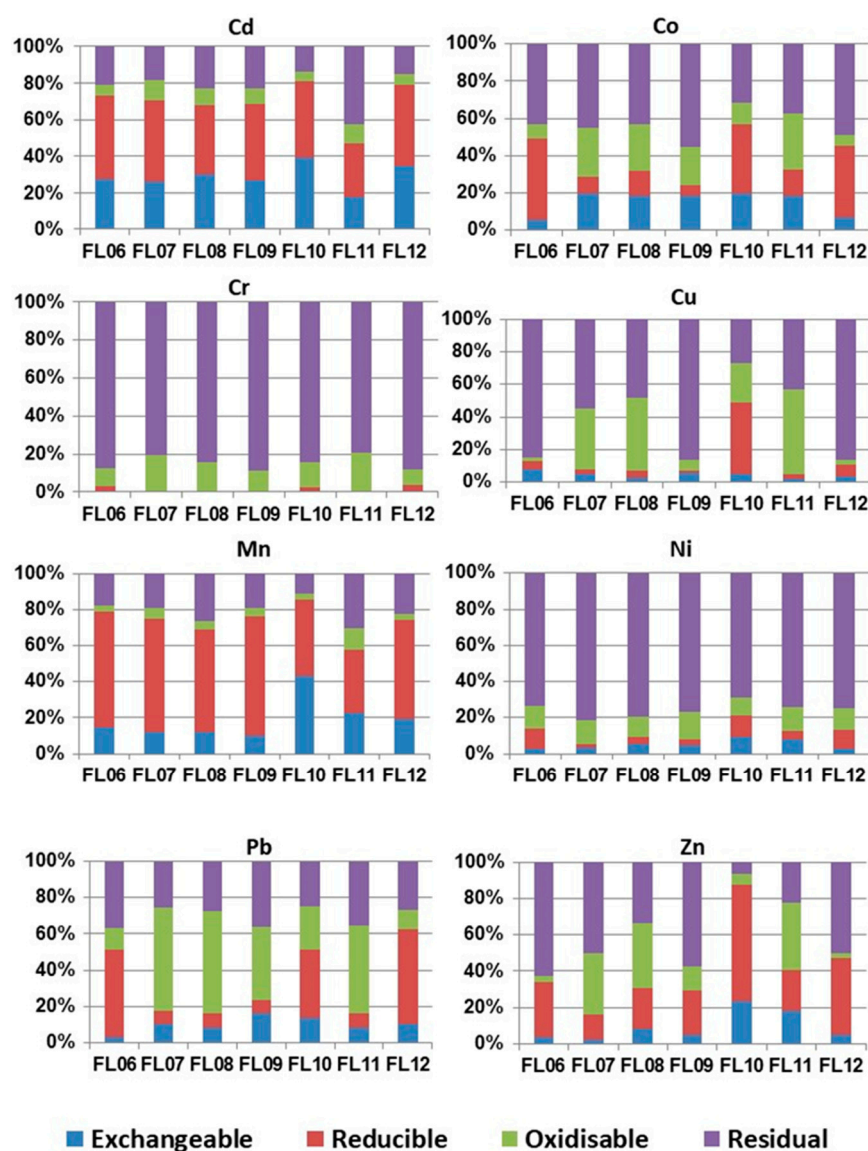


Figure 6. Geochemical fractionation of the investigated trace elements according to the modified BCR sequential extraction protocol.

The reactive trace elements concentrations in the same 7 samples, determined by using the 0.43 M HNO₃ extraction represents the fraction of metals that is available for environmental mobilization and therefore is relevant to human health risks. The proportion of reactive elements in the studied samples, expressed as the percentage of the concentration that is extracted by aqua regia is presented in the boxplots of Figure 7.

Zinc presented a wide range of percentages, varying from 35% up to 100% of total content across the sampling points. Additionally, Cd ratios also covered a wide range, from 55% to 100%, indicating that the proportion of the reactive phases' pool of this element is not controlled solely by the total Cd content. Furthermore, Pb, Cu, Mn and Co presented high medians and a wide variation concerning the percentages of dilute HNO₃ over aqua regia ranging from 42% to 87% of total content. Contrarily, significantly lower percentage medians and variation were estimated for Ni and Cr, i.e., below 30% for all samples.

Regarding the seasonal variation in reactive elemental concentrations, significant differences (ANOVA, $p < 0.05$) between the first sampling, 3 weeks after the flood and samplings during the following months were observed only for Cd and Mn (Figure 8). It is noted that measurements of TOC in the respective samples immediately after the flood also yielded significantly higher values compared to the following seasons of the year.

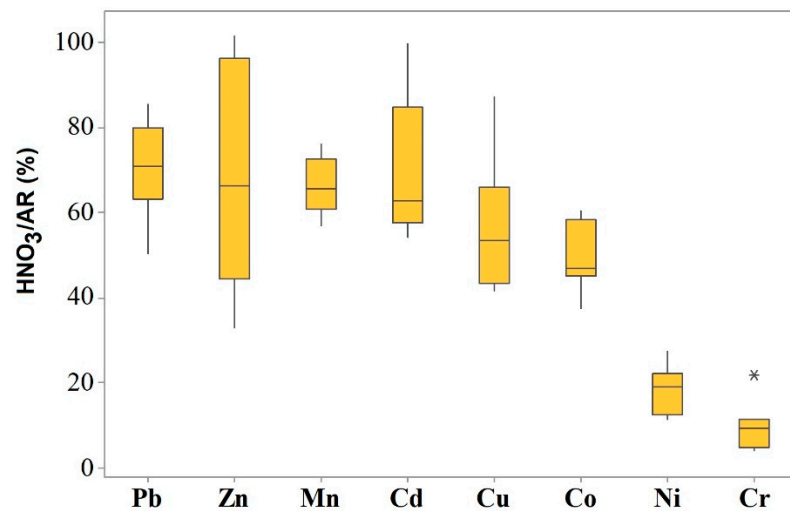


Figure 7. Boxplots of the proportions of reactive elements, expressed as ratios of dilute nitric acid-extracted over aqua regia-extracted concentrations ($n = 7$).

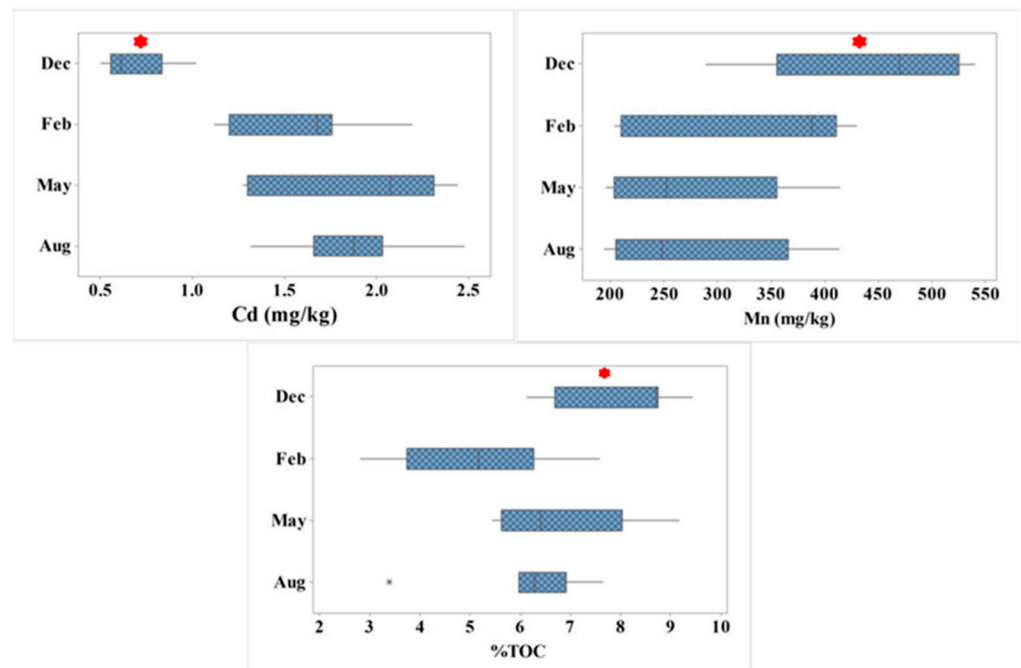


Figure 8. Boxplots of reactive concentrations of Cd and Mn and TOC measured in 7 samples collected seasonally along T2 in the flood affect area. Red stars indicate a statistically significant difference in the first set of samples, collected 3 weeks after the flash flood event.

3.4. Spatial Distribution of Trace Elements and other Measured Parameters

The spatial distribution of aqua regia extractable concentrations of the studied trace elements, plotted by using graduated size symbols, are presented in Figure 9. Distinct differences in the distribution pattern of the elements are observed, with the highest concentrations of Pb, Cu and Zn observed in samples collected after the flood along T2 which crosses the industrial area of Mandra town. Specifically, statistically significant higher concentrations in T2 were estimated for Pb and Zn (ANOVA, $p < 0.05$). Contrarily, Cr, As, Mn, Ni and Co presented a more homogeneous distribution in the sampling area, without noticeable differences in sampling points from the industrial area. The statistical summary of concentration data for all studied trace elements is provided in Table S2 and the spatial patterns of other measured parameters, i.e., pH, %TOC and χ are presented in

Figure S3. Of these parameters, only χ seems to follow the pattern of the first group of trace elements with higher values in samples from the industrial area.

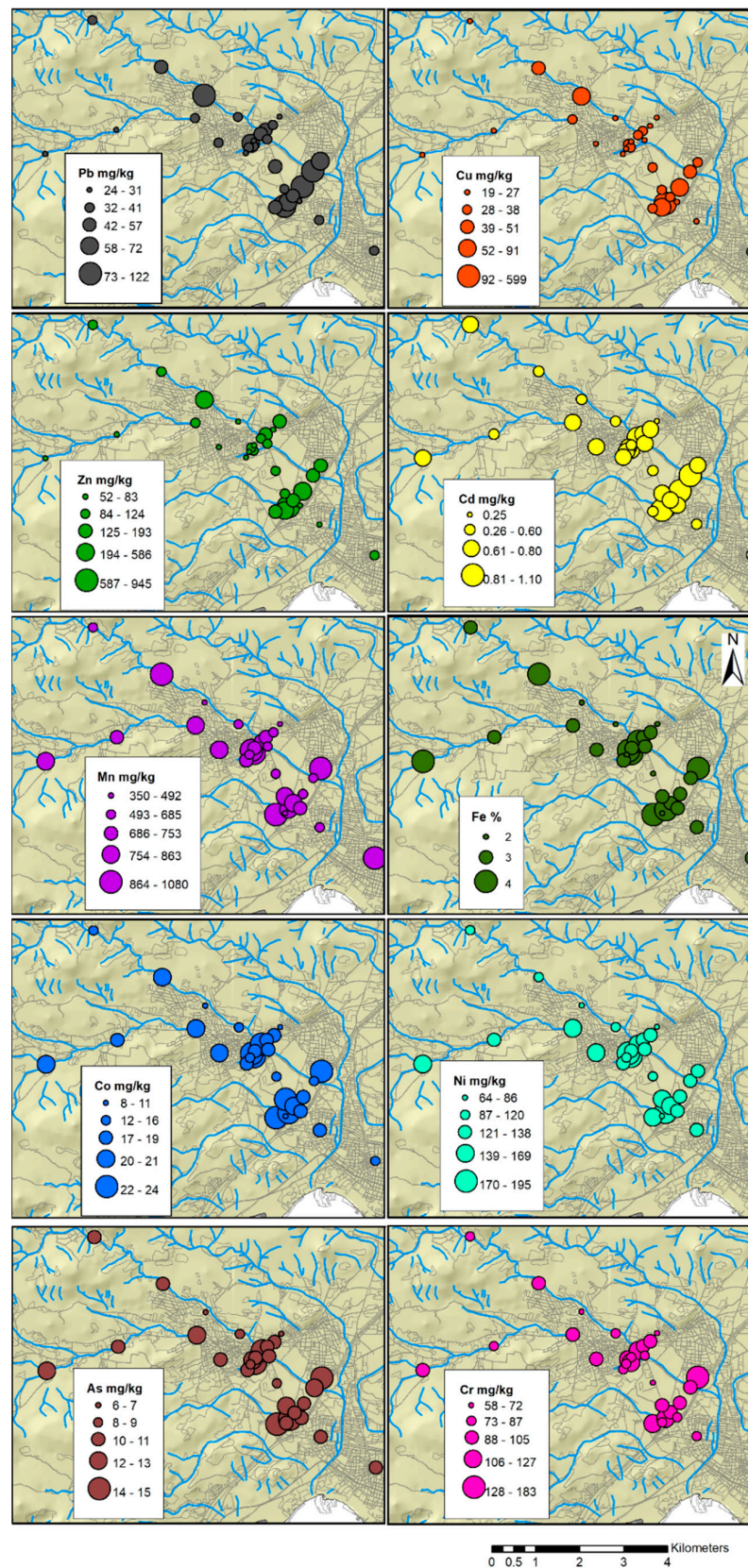


Figure 9. Spatial distribution of aqua regia extracted concentrations of trace elements in the study area.

4. Discussion

4.1. Natural versus Anthropogenic Sources of Trace Elements

While the atmospheric fluxes onto impervious urban surfaces may significantly contribute to the contamination of urban runoff and play an important role in elemental cycling in the urban environment [47], the dominating process in the study area has been the influx of eroded material from upstream during the flash flood event. This is evidenced by the higher enrichment in $Cr > Ni > Mn > Fe$ in the flood deposited material, compared to the adjacent Thriassio soils based on the previous study by Massas et al. [30], as well as the grouping of measured parameters according to the multivariate techniques applied.

Specifically, the cluster analysis results show a distinct classification of the elements according to their origin. Arsenic, Co, Cr, Fe, Mn and Ni were significantly positively correlated to clay content, providing evidence that these elements were mainly of geogenic origin and dominant in the flood deposited sediment. Cadmium, Cu, Pb and Zn are grouped in a separate cluster which also contains magnetic susceptibility (χ). The trace elements of this latter cluster are typical anthropogenic contaminants [30,48–50].

The above associations are further supported by the results of factor analysis. The positive loadings of the first group of elements indicate that the major controlling factor is their common geogenic origin from upstream eroded material. Furthermore, a strong positive correlation is observed between Al and Fe (Figure S4) in the collected samples, indicative of the influence of the geological background to the chemical composition of the flood-deposited sediment. Bauxite occurrences in the area are a potential source of this group of trace elements. Although detailed literature information on trace element contents of bauxite occurrences from the study area is lacking, other bauxitic laterite deposits of Central Greece have been studied in the past in this respect [32]. These deposits are lying on similar geology i.e., on karstified Triassic–Jurassic limestone, and are conformably overlain by Lower Cretaceous limestone. They occur either as isolated typical Ni or bauxitic–laterite ores or as an association of Fe–Ni ore at the lower part of the deposit, followed by bauxitic–laterite towards its upper part and are characterized by exceptionally high As, Cr and Co contents. Arsenates were found to occur as sorbed species onto goethite-type phases in the bauxitic laterites of Central Greece [51]. Terra rossa, a reddish clayey to silty–clayey soil especially widespread in the Mediterranean region, which covers limestone and dolomite, is also present in the study area. Terra rossa may have formed exclusively from the insoluble residue of limestone and dolomite but often comprises a span of parent materials which arrived on the carbonate terrain via different transport mechanisms [52]. Typical minerals of Mediterranean terra rossa including carbonates (calcite, dolomite) and aluminosilicate minerals (illite and chlorite) were identified in samples of the present study (Figure 2). The typical red color of the material is due to Fe oxides, present as hematite and goethite effectively acting as sorption surfaces of trace elements.

Regarding the spatial distribution of trace elements, significantly higher concentrations of Pb and Zn were observed in T2 which crosses the industrial area of Mandra town. This indicates that the accumulation of these PTEs in the depositional sediments is considerably influenced by automobile traffic and industrial facilities. The potential sources of these metals include vehicle emissions from the dense network of roads and can be tied to automobile byproducts. Additional sources of these elements in an urban environment can be incinerators, pipes, cables, and paints [53]. However, the possibility that a proportion of some trace elements of mainly geogenic origin such as As and Cr is influenced by anthropogenic sources, especially within the industrial area of Mandra, cannot be excluded.

4.2. Trace Element Fractionation in Flood Sediments and Seasonal Variation

Undoubtedly a more relevant indicator for assessing the health risk for humans and the ecosystem after the flood is the fractionation of trace elements in easily mobilizable forms, which can trigger exposure to PTEs. In this respect, the modified BCR method results provided a clear indication of the most susceptible trace elements to mobilization in the order $Cd > Mn > Pb > Co > Ni > Cr$. The results of sequential extraction for Zn and

Cu were not consistent between the analyzed samples, probably indicating involvement of very site-specific conditions in the control of their speciation. Furthermore, the notable fractionation of Cr and Ni in the residual phase signifies the presence of Cr-spinels and Ni-bearing silicate lattices, such as serpentine and smectite minerals, as a major structural component in the analyzed samples. This is supporting the hypothesis of the upstream eroded soil being the major contribution to the flood deposited sediments. Indeed, soils of the wider region upstream with similar bedrock geology are rich in such minerals as found in previous studies at the area of Thiva [54,55].

Reactivity ratios, involving data from the dilute HNO₃ extraction, are also used as metal availability indices since they correspond to the percentage reactive fraction of metal's total concentration in soil. This reduces the influence of the geogenic factor on these environmental availability indicators and makes them more sensitive to anthropogenic pollution sources. The availability of metals in soils is mainly influenced by the clay and total organic carbon content, the pH, and the composition of the soils' parent material. This could differentiate the estimated reactive percentages of trace elements in different soils even under the same land use pattern and total metal amounts [30]. Reactivity ratios depend on the proportion of the mobilizable phases in the given soil matrix; the higher the ratio, the higher the proportion of the host phases that are susceptible to dissolution by the given reagent [56]. In the present study the highest reactivity ratios, reaching values over 90%, have been observed for Zn, Cd, Pb, Cu, Mn and Co extracted by dilute HNO₃ over total content extracted by aqua regia. The same trend was observed for most of these elements as estimated by the modified BCR extraction analysis; thus, those trace elements are the most vulnerable to mobilization in the flood runoff.

The lower concentrations of Cd during the December sampling period, 3 weeks after the flood, signify that many cadmium compounds found either in atmospheric dust or in effluents of principal sources, such as cadmium sulfate and cadmium chloride that are quite soluble in water, were probably washed out by the flood [57]. However, the significantly higher concentrations of Mn during the December sampling period might reflect the flood event and the load-bearing materials and volumes of soil drifted by the flood. Further research entailing soil coring is necessary to be able to assess the downwards migration of PTEs and possible infiltration into the aquifer. Furthermore, research gaps to be addressed in similar events in the future include further modelling of relationships between extreme events and health impacts; improved understanding of factors affecting vulnerability to climate extremes; and assessment of the effectiveness of adaptation in different settings [58].

5. Conclusions

Increasing frequency or severity of some extreme weather events, such as extreme precipitation, flooding, droughts, and storms, threaten the health of people during and after such events [15]. Extreme precipitation events due to environmental change are expected to become more frequent in the future, however, their effects on health are difficult to quantify, because secondary and delayed consequences are poorly reported. The flash flood in Mandra is a typical example of this type of natural disaster with possible long-term effects, possibly affecting human and ecosystem health. The present study provided insight into potential factors affecting the origin and fractionation of trace elements in flood deposited sediments and their further dispersion in the surface environment by successfully applying a set of analytical techniques that proved effective in providing relevant information.

An enrichment of Cr > Ni > Mn > Fe in the flood-deposited material compared to the local soil geochemical baseline has been identified, indicating that the major contribution to the chemistry of flood deposits was the upstream eroded material. Furthermore, the flood has resulted in remobilization of some elements in the surface cover and their sequestration in environmentally mobile phases as evidenced by the elevated concentrations of trace elements such as Pb and Zn in the flooded industrial area of Mandra. Regarding the elemental fractionation in the flood sediments, the high percentage (40%) of Cd in the operationally defined exchangeable fraction, suggests that this PTE is the most susceptible

to mobilization during runoff. High reactivity ratios, reaching values of over 90%, have been observed for Cd, and Zn, indicating vulnerability of both PTEs to mobilization, should the physicochemical conditions of the soil cover change. There was a significant seasonal variation of TOC, Cd and Mn in the months following the flood, whereas no significant difference was observed for the other studied PTEs. The results of the present study provide an objective basis for better management of the risks related to exposure of inhabitants to contaminated flood deposited sediments in areas of similar characteristics.

Supplementary Materials: The following are available online at <https://www.mdpi.com/article/10.3390/su14042448/s1>, Figure S1: Photographs from the sampling area, Figure S2: Simplified lithological map of the area, Figure S3: spatial distribution of pH, %TOC and χ in the sampling area, Figure S4: Correlation between Al and Fe in collected samples, Table S1: Results of SEM-EDS microanalysis, Table S2: Comparison of trace element concentrations in samples of the two traverses.

Author Contributions: Conceptualization, A.A. and P.M.K.; methodology, A.A., P.M.K. and E.K.; formal analysis, P.M.K., V.P. and F.B.; investigation, P.M.K., A.A. E.K.; resources, P.M.K., A.A. and M.D.; data curation, P.M.K. and V.P.; writing—original draft preparation, P.M.K.; writing—review and editing, A.A., V.P., F.B., E.K., and M.D.; visualization, P.M.K. and A.A.; supervision, A.A.; project administration, A.A.; funding acquisition, P.M.K. and A.A. All authors have read and agreed to the published version of the manuscript.

Funding: This research was funded by the Hellenic Foundation for Research and Innovation (HFRI) and the General Secretariat for Research and Technology (GSRT), under the HFRI PhD Fellowship grant (GA. No. 1225/14677).

Data Availability Statement: Data supporting reported results are available from the paper authors upon request.

Acknowledgments: The postgraduate students of the course “Environmental Management- Mineral Resources” of NKUA, class of 2017-2018 are acknowledged for their help during field sampling and laboratory sample preparation. Zacharenia Kypritidou is acknowledged for helping with mineralogical identification of P-XRD patterns. We thank the two anonymous reviewers for their constructive comments that improved the quality of the manuscript.

Conflicts of Interest: The authors declare no conflict of interest. The funders had no role in the design of the study; in the collection, analyses, or interpretation of data; in the writing of the manuscript, or in the decision to publish the results.

References

1. Diakakis, M.; Andreadakis, E.; Nikolopoulos, E.I.; Spyrou, N.I.; Gogou, M.E.; Deligiannakis, G.; Antoniadis, Z. An integrated approach of ground and aerial observations in flash flood disaster investigations. The case of the 2017 Mandra flash flood in Greece. *Int. J. Dis. Risk Red.* **2018**, *33*, 290–309. [[CrossRef](#)]
2. Merz, B.; Kreibich, H.; Schwarze, R.; Thielen, A. Assessment of economic flood damage. *Nat. Hazards Earth Syst. Sci.* **2010**, *10*, 1697–1724. [[CrossRef](#)]
3. Diakakis, M.; Deligiannakis, G.; Katsetsiadou, K.; Antoniadis, Z.; Melaki, M. Mapping and classification of direct flood impacts in the complex conditions of an urban environment. The case study of the 2014 flood in Athens, Greece. *Urban Water J.* **2017**, *14*, 1065–1074. [[CrossRef](#)]
4. Barredo, J.I. Major flood disasters in Europe: 1950–2005. *Nat. Hazards* **2007**, *42*, 125–148. [[CrossRef](#)]
5. Barredo, J.I. Normalised flood losses in Europe: 1970–2006. *Nat. Hazards Earth Syst. Sci.* **2009**, *9*, 97–104. [[CrossRef](#)]
6. Llasat, M.C.; Llasat-Botija, M.; Prat, M.A.; Porcu, F.; Price, C.; Mugnai, A.; Yair, Y. High-impact floods and flash floods in Mediterranean countries: The FLASH preliminary database. *Adv. Geosci.* **2010**, *23*, 47–55. [[CrossRef](#)]
7. Petersen, M.S. Impacts of flash floods. In *Coping with Flash Floods*; Springer: Dordrecht, The Netherlands, 2001; Volume 77, pp. 11–13. [[CrossRef](#)]
8. Dumas, C.; Aubert, D.; Durrieu de Madron, X.; Ludwig, W.; Heussner, S.; Delsaut, N.; Menniti, C.; Sotin, C.; Buscail, R. Storm-induced transfer of particulate trace metals to the deep-sea in the Gulf of Lion (NW Mediterranean Sea). *Environ. Geochem. Health* **2014**, *36*, 995–1014. [[CrossRef](#)]
9. Diakakis, M.; Mavroulis, S.; Deligiannakis, G. Floods in Greece, a statistical and spatial approach. *Nat. Hazards* **2012**, *62*, 485–500. [[CrossRef](#)]

10. Diakakis, M.; Deligiannakis, G.; Andreadakis, E.; Katsetsiadou, K.N.; Spyrou, N.I.; Gogou, M.E. How different surrounding environments influence the characteristics of flash flood-mortality: The case of the 2017 extreme flood in Mandra, Greece. *J. Flood Risk Manag.* **2020**, *13*, e12613. [[CrossRef](#)]
11. Müller, A.; Wessels, M. The flood in the Odra River 1997—Impact of suspended solids on water quality. *Acta Hydroch. Et Hydrobiol.* **1995**, *27*, 316–320. [[CrossRef](#)]
12. Karkani, A.; Evelpidou, N.; Tzouanioti, M.; Petropoulos, A.; Santangelo, N.; Hampik Maroukian, H.; Spyrou, E.; Lakidi, L. Flash Flood Susceptibility Evaluation in Human-Affected Areas Using Geomorphological Methods—The Case of 9 August 2020, Euboea, Greece. A GIS-Based Approach. *GeoHazards* **2021**, *2*, 366–382. [[CrossRef](#)]
13. Baborowski, M.; Von Tümpling, W., Jr.; Friese, K. Behaviour of suspended particulate matter (SPM) and selected trace elements during the 2002 summer flood in the River Elbe (Germany) at Magdeburg monitoring station. *Hydrol. Earth Syst. Sci. Dis. Eur. Geosci. Union* **2004**, *8*, 135–150. [[CrossRef](#)]
14. Alfieri, L.; Burek, P.; Feyen, L.; Forzieri, G. Global warming increases the frequency of river floods in Europe. *Hydrol. Earth Syst. Sci.* **2015**, *19*, 2247–2260. [[CrossRef](#)]
15. USGCRP. *The Impacts of Climate Change on Human Health in the United States: A Scientific Assessment*; Crimmins, A., Balbus, J., Gamble, J.L., Beard, C.B., Bell, J.E., Dodgen, D.R.J., Eisen, R.J., Fann, N., Hawkins, M.D., Hawkins, S.C., et al., Eds.; U.S. Global Change Research Program: Washington, DC, USA, 2016; p. 312. [[CrossRef](#)]
16. Coynel, A.; Schäfer, J.; Blanc, G.; Bossy, C. Scenario of particulate trace metal and metalloid transport during a major flood event inferred from transient geochemical signals. *Appl. Geochem.* **2007**, *22*, 821–836. [[CrossRef](#)]
17. Coynel, A.; Schäfer, J.; Dabrin, A.; Girardot, N.; Blanc, G. Groundwater contributions to metal transport in a small river affected by mining and smelting waste. *Water Res.* **2007**, *41*, 3420–3428. [[CrossRef](#)] [[PubMed](#)]
18. Resongles, E.; Casiot, C.; Freydier, R.; Le Gall, M.; Elbaz-Poulichet, F. Variation of dissolved and particulate metal(loid) (As, Cd, Pb, Sb, Tl, Zn) concentrations under varying discharge during a Mediterranean flood in a former mining watershed, the Gardon River (France). *J. Geochem. Explor.* **2015**, *158*, 132–142. [[CrossRef](#)]
19. Ciszewski, D.; Grygar, T.M. A Review of Flood-Related Storage and Remobilization of Heavy Metal Pollutants in River Systems. *Water Air Soil Pollut.* **2016**, *227*, 239. [[CrossRef](#)] [[PubMed](#)]
20. Matys Grygar, T.; Elznicová, J.; Bábek, O.; Hošek, M.; Engel, Z.; Kiss, T. Obtaining isochrones from pollution signals in a fluvial sediment record: A case study in a uranium-polluted floodplain of the Ploučnice River, Czech Republic. *Appl. Geochem.* **2014**, *48*, 1–15. [[CrossRef](#)]
21. Alderman, K.; Turner, L.R.; Tong, S. Floods and human health: A systematic review. *Environ. Int.* **2012**, *47*, 37–47. [[CrossRef](#)]
22. Kelly, T.J.; Hamilton, E.; Watts, M.J.; Ponting, J.; Sizmur, T. The Effect of Flooding and Drainage Duration on the Release of Trace Elements from Floodplain Soils. *Environ. Tox. Chem.* **2020**, *39*, 2124–2135. [[CrossRef](#)]
23. Su, T.; Shu, S.; Shi, H.; Wang, J.; Adams, C.; Witt, E.C. Distribution of toxic trace elements in soil/sediment in post-Katrina New Orleans and the Louisiana Delta. *Environ. Pollut.* **2008**, *156*, 944–950. [[CrossRef](#)] [[PubMed](#)]
24. Škrbić, B.D.; Živančev, J.; Antić, I.; Buljovčić, M. Pollution status and health risk caused by heavy elements in the flooded soil and vegetables from typical agricultural region in Vojvodina Province, Serbia. *Environ. Sci. Pollut. Res.* **2021**, *28*, 16065–16080. [[CrossRef](#)] [[PubMed](#)]
25. Abgottsporn, F.; Bigalke, M.; Wilcke, W. Fast colloidal and dissolved release of trace elements in a carbonatic soil after experimental flooding. *Geoderma* **2015**, *259–260*, 156–163. [[CrossRef](#)]
26. Coates-Marnane, J.; Olley, J.; Burton, J.; Grinham, A. The impact of a high magnitude flood on metal pollution in a shallow subtropical estuarine embayment. *Sci. Total Environ.* **2016**, *569–570*, 716–731. [[CrossRef](#)]
27. Kanellopoulos, T.D.; Karageorgis, A.P.; Kikaki, A.; Chourdaki, S.; Hatzianestis, I.; Vakalas, I.; Hatiris, G.A. The impact of flash-floods on the adjacent marine environment: The case of Mandra and Nea Peramos (November 2017), Greece. *J. Coast. Cons.* **2020**, *24*, 56. [[CrossRef](#)]
28. Robertson, D.J.; Taylor, K.G.; Hoon, S.R. Geochemical and mineral magnetic characterisation of urban sediment particulates, Manchester, UK. *Appl. Geochem.* **2003**, *18*, 269–282. [[CrossRef](#)]
29. Adams, C.; Witt, E.C.; Wang, J.; Shaver, D.K.; Summers, D.; Filali-Meknassi, Y.; Shi, H.; Luna, R.; Anderson, N. Chemical Quality of Depositional Sediments and Associated Soils in New Orleans and the Louisiana Peninsula Following Hurricane Katrina. *Environ. Sci. Technol.* **2007**, *41*, 3437–3443. [[CrossRef](#)]
30. Massas, I.; Kalivas, D.; Ehaliotis, C.; Gasparatos, D. Total and available heavy metal concentrations in soils of the Thriassio plain (Greece) and assessment of soil pollution indexes. *Environ. Monit. Assess.* **2013**, *185*, 6751–6767. [[CrossRef](#)]
31. Dounas, A.G. The Geology of the Area between Megara and Erithrai Village (Attica). Ph.D. Thesis, School of Physical Sciences, National and Kapodistrian University of Athens, Athens, Greece, 1971; p. 185. (In Greek)
32. Eliopoulos, D.G.; Economou-Eliopoulos, M. Geochemical and mineralogical characteristics of Fe–Ni and bauxitic-laterite deposits of Greece. *Ore Geol. Rev.* **2000**, *16*, 41–58. [[CrossRef](#)]
33. Deligiannakis, G.; Papanikolaou, D.; Roberts, G. Fault specific GIS based seismic hazard maps for the Attica region, Greece. *Geomorphology* **2018**, *306*, 264–282. [[CrossRef](#)]
34. Argyraki, A. Garden soil and house dust as exposure media for lead uptake in the mining village of Stratoni, Greece. *Environ. Geochem. Health* **2014**, *36*, 677–692. [[CrossRef](#)] [[PubMed](#)]

35. ISO 10390. Soil Quality-Determination of pH. 1994. Available online: <https://www.iso.org/standard/18454.html> (accessed on 17 February 2022).
36. Hoogsteen, M.J.J.; Lantinga, E.A.; Bakker, E.J.; Groot, J.C.J.; Tittonell, P.A. Estimating soil organic carbon through loss on ignition: Effects of ignition conditions and structural water loss. *Eur. J. Soil Sci.* **2015**, *66*, 320–328. [[CrossRef](#)]
37. Thompson, R.; Oldfield, F. *Environmental Magnetism*; Allen and Unwin: London, UK, 1986. [[CrossRef](#)]
38. Bouyoucos, G.H. A recalibration of the hydrometer method for making mechanical analysis of soils. *Agron. J.* **1951**, *43*, 434–438. [[CrossRef](#)]
39. Luo, X.-S.; Yu, S.; Li, X.-D. Distribution, availability, and sources of trace elements in different size fractions of urban soils in Hong-Kong: Implications for assessing the risk to human health. *Environ. Pollut.* **2011**, *159*, 1317–1326. [[CrossRef](#)] [[PubMed](#)]
40. Rauret, G.; López-Sánchez, J.F.; Sahuquillo, A.; Rubio, R.; Davidson, C.; Ure, A.M.; Quevauviller, P. Improvement of the BCR three step sequential extraction procedure prior to the certification of new sediment and soil reference materials. *J. Environ. Monit.* **1999**, *1*, 57–61. [[CrossRef](#)] [[PubMed](#)]
41. Rodrigues, S.M.; Henriques, B.; Ferreira da Silva, E.; Pereira, M.E.; Duarte, A.C.; Romkens, P.F.A.M. Evaluation of an approach for the characterization of reactive and available pools of twenty potentially toxic elements in soils: Part I—The role of key soil properties in the variation of contaminants' reactivity. *Chemosphere* **2010**, *81*, 1549–1559. [[CrossRef](#)] [[PubMed](#)]
42. European Union. Copernicus Land Monitoring Service 2018. European Environment Agency (EEA). Available online: <https://land.copernicus.eu/pan-european/corine-land-cover/clc2018> (accessed on 17 February 2022).
43. Manly, B.F.J. *Multivariate Statistical Methods, a Primer*; Chapman & Hall: London, UK, 1994. [[CrossRef](#)]
44. Bourliva, A.; Papadopoulou, L.; Aidona, E.; Giouri, K.; Simeonidis, K.; Vourlias, G. Characterization and geochemistry of technogenic magnetic particles (TMPs) in contaminated industrial soils: Assessing health risk via ingestion. *Geoderma* **2017**, *295*, 86–97. [[CrossRef](#)]
45. Pérez-López, R.; Álvarez-Valero, A.M.; Nieto, J.M.; Sáez, R.; Matos, J.X. Use of sequential extraction procedure for assessing the environmental impact at regional scale of the São Domingos Mine (Iberian Pyrite Belt). *Appl. Geochem.* **2008**, *23*, 3452–3463. [[CrossRef](#)]
46. Madrid, F.; Reinoso, R.; Florido, M.C.; Díaz Barrientos, E.; Ajmone-Marsan, F.; Davidson, C.M.; Madrid, L. Estimating the extractability of potentially toxic metals in urban soils: A comparison of several extracting solutions. *Environ. Pollut.* **2007**, *147*, 713–722. [[CrossRef](#)]
47. Garnaud, S.; Mouchel, J.M.; Chebbo, G.; Thévenot, D.R. Heavy metal concentrations in dry and wet atmospheric deposits in Paris district: Comparison with urban runoff. *Sci. Total Environ.* **1999**, *235*, 235–245. [[CrossRef](#)]
48. Moller, A.; Muller, H.W.; Abdullah, A.; Abdelgawad, G.; Utermann, J. Urban soil pollution in Damascus, Syria: Concentrations and patterns of heavy metals in the soils of the Damascus Ghouta. *Geoderma* **2005**, *124*, 63–71. [[CrossRef](#)]
49. Ljung, K.; Otabbong, E.; Selinus, O. Natural and anthropogenic metal inputs in urban Uppsala, Sweden. *Environ. Geochem. Health* **2006**, *28*, 353–364. [[CrossRef](#)]
50. Yaylali-Abanuz, G. Heavy metal contamination of surface soil around Gebze industrial area, Turkey. *Microchem. J.* **2011**, *99*, 82–92. [[CrossRef](#)]
51. Gamaletsos, P.N.; Kalatha, S.; Godelitsas, A.; Economou-Eliopoulos, M.; Göttlicher, J.; Steininger, R. Arsenic distribution and speciation in the bauxitic Fe-Ni-laterite ore deposit of the Patitira mine, Lokris area (Greece). *J. Geochem. Explor.* **2018**, *194*, 189–197. [[CrossRef](#)]
52. Durn, G. Terra Rossa in the Mediterranean Region: Parent Materials, Composition and Origin. *Geol. Croat.* **2003**, *56*, 83–100.
53. Seleznev, A.A.; Yarmoshenko, I.V. Study of urban puddle sediments for understanding heavy metal pollution in an urban environment. *Environ. Technol. Innov.* **2014**, *1–2*, 1–7. [[CrossRef](#)]
54. Kelepertzis, E.; Galanos, E.; Mitsis, I. Origin, mineral speciation and geochemical baseline mapping of Ni and Cr in agricultural topsoils of Thiva valley (central Greece). *J. Geochem. Explor.* **2013**, *125*, 56–68. [[CrossRef](#)]
55. Kelepertzis, E.; Stathopoulou, E. Availability of geogenic heavy metals in soils of Thiva town (central Greece). *Environ. Monit. Assess.* **2013**, *185*, 9603–9618. [[CrossRef](#)] [[PubMed](#)]
56. Argyraki, A.; Kelepertzis, E.; Botsou, F.; Paraskevopoulou, V.; Katsikis, I.; Trigoni, M. Environmental availability of trace elements (Pb, Cd, Zn, Cu) in soil from urban, suburban, rural and mining areas of Attica, Hellas. *J. Geochem. Explor.* **2018**, *187*, 201–213. [[CrossRef](#)]
57. Nriagu, J.O. (Ed.) Global cadmium cycle. In *Cadmium in the Environment*; Wiley: New York, NY, USA; Chichester, UK; Brisbane, Australia; Toronto, ON, Canada; Singapore, 1994; pp. 1–12.
58. WHO; McMichael, A.J.; Campbell-Lendrum, D.H.; Corvalán, C.F.; Ebi, K.L.; Githeko, A.K.; Scheraga, J.D. Climate Change and Human Health: Risks and Responses-SUMMARY. 2003. Available online: <https://www.who.int/globalchange/environment/en/ccSCREEN.pdf?ua=1> (accessed on 17 February 2022).